Research Article

Ding Renwei, Liu Handong, Yuan Guangxiang, and Dong Jinyu*

Deformation and Subsidence prediction on Surface of Yuzhou mined-out areas along Middle Route Project of South-to-North Water Diversion, China

https://doi.org/10.1515/geo-2018-0065
Received Feb 06, 2018; accepted Oct 17, 2018

Abstract: The Middle Route of the South-to-North Water Diversion Project crosses the coal mined-out area in Yuzhou city. There are 4 mined-out areas along Yuzhou section of the water diversion project. The collapse, fracture and deformation of overlying rock mass occurred due to strata loss and stress field change, which then resulted in the subsidence, collapse fissures on the ground. The deformation of the upper rock mass is characterized by "three-zone": caving zone, fault zone, and bend zone. Thus, it is very important to predict the surface subsidence of the mined-out areas. Highly precise deformation observation network were set along the channel. The monitoring data show that the surface tilt, curvature and horizontal deformation of the mined-out areas were less than critical values. However, the forecast and monitoring values are relatively larger in Guocun and Xinfeng mined-out areas due to large mining range and the possible location of two mined-out areas in the affected region. Therefore, the monitoring should focus on the two mined-out areas.

Keywords: middle route project of south-to-north water diversion; mined-out area; deformation of surface; subsidence prediction

***Corresponding Author: Dong Jinyu:** College of Geosciences and Engineering, North China University of Water Resources and Electric Power, Zhengzhou, China; Email: dongjinyu@ncwu.edu.cn
Ding Renwei: College of Geosciences and Engineering, North China University of Water Resources and Electric Power, Zhengzhou, China; Email: dingrenwei2017@126.com
Liu Handong: College of Geosciences and Engineering, North China University of Water Resources and Electric Power, Zhengzhou,China, Email: liuhandong@ncwu.edu.cn
Yuan Guangxiang: College of Geosciences and Engineering, North China University of Water Resources and Electric Power, Zhengzhou,China, Email: yuhuaichang@ncwu.edu.cn

1 Introduction

Underground mining activities cause movement both in geological strata and on the ground surface. Deformation and Subsidence as a result of underground mining is a hazard to human life, properties and environment. Before 1889, there are reports about subsidence of ground surface caused by underground mining activities [1]. Can, *et al.* identified the effects of mining subsidence on masonry buildings in the mining area of Kozlu, Zonguldak, Turkey and detailed the results from a GPS Network conducted in the basin to determine the horizontal displacements on the surface created by the mining activities [2, 3]. Donnelly *et al.* reported that long wall mining methods resulted in subsidence that has caused severe damage to structures, residential property, and agricultural land, and also induced landslides in the Amaga, Angelopolis, Venecia and Bolombolo Regions, Antioquia, Colombia, and the "Subsidence with Influence Function Technique" program was used to predict the magnitude of subsidence [4]. Gayarre, *et al.* presented a forensic analysis of ground subsidence in Lo Tacón industrial area, which is located at the outskirts of La Unión (Murcia, SE Spain) [5]. The subsidence was triggered by the collapse of abandoned underground mining caverns occurred in 1998. Nádudvariused radar interferometer and SBAS technique were used to detect surface subsidence relating to coal mining in Upper Silesia from the periods of 1993-2000 and 2003-2010 [6]. Howladar & Hasan evaluated the development of subsidence caused by the extraction of 1203 slice under the profile functions and influence functions methods [7]. Jung, *et al.* developed a quick, simple and quantitative method suitable for the estimation of subsidence susceptibility prior to the detailed field investigation of coal mines in Korea [8]. Hu, *et al.* got a few phases of measured data based on the long-term dynamic monitoring, and revealed the surface movement and deformation characteristics in the typical windy and sandy region in Bulianta coal mine of Shendong coal-

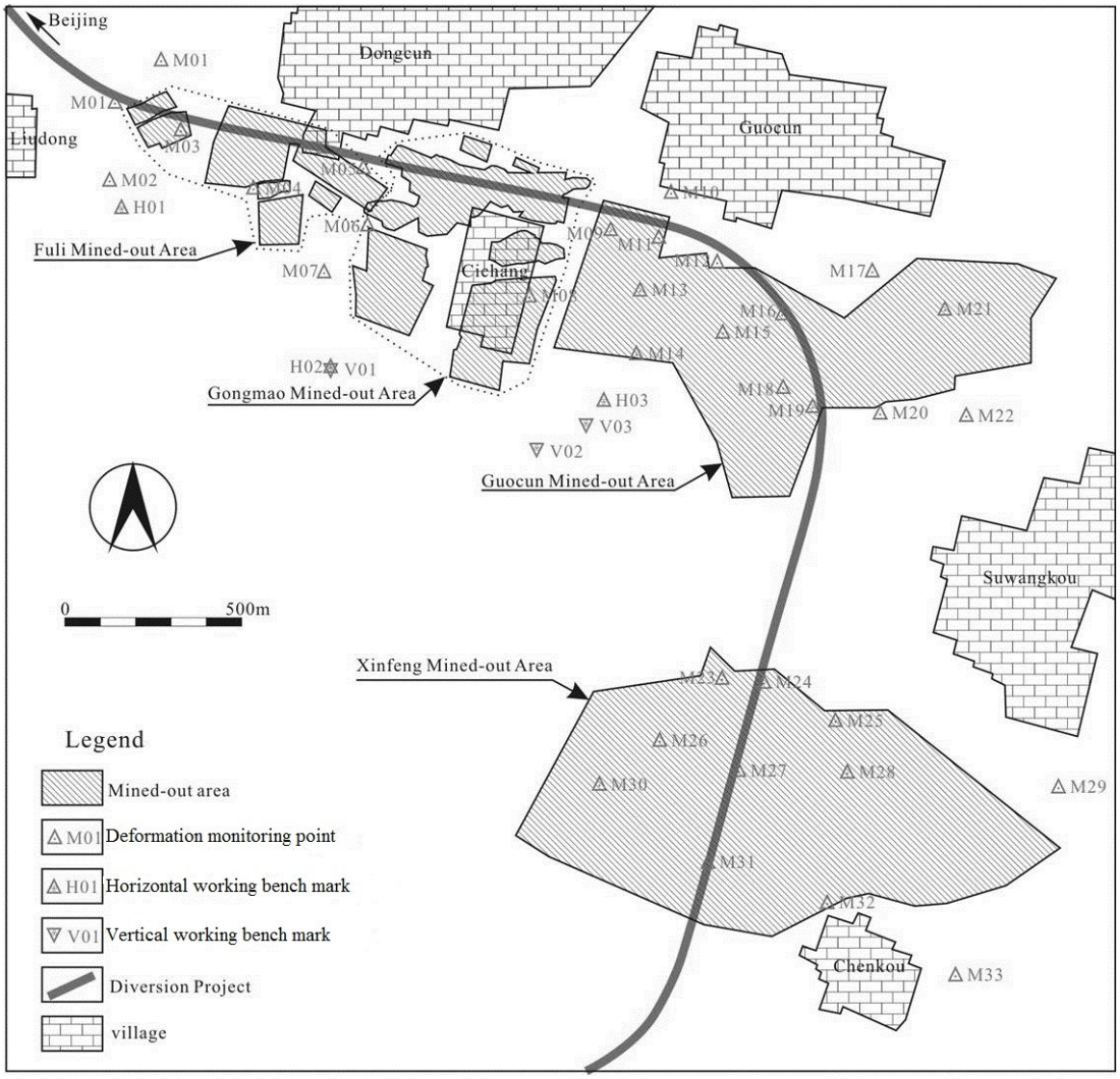

Figure 1: Schematic layout of mined-out areas along Yuzhou section of the Diversion Project.

field, located in Ordos, Inner Mongolia [9]. Sun, *et al.* investigated the formation mechanism, relevant influential factors, and distribution laws of the collapse in the third mining area in Gongchangling District, Liaoyang City, China, and conducted evaluation and prediction of ground settlement induced by the goaf collapse [10]. Li, *et al.* used a similar material simulation method to examine the influencing mechanism(s) of abandoned goafs on the subsidence basin in the Nan Tun coal mine, Yanzhou, China [11].

The 1,277km long Middle Route of the South-to-North Water Diversion Project conveys water from Danjiangkou reservoir in the middle and upper reaches of Hanjiang River to Henan, Hebei, Beijing, and Tianjin through open canal. The route crosses the coal mining area in Yuzhou City, Henan Province, with 3.11km long goaf. Thus, the stability of goaf is one of the major technical problems in Yuzhou section of the Middle Route of the South-to-North Water Diversion Project [12, 13].

2 The description and geology of the research site

2.1 Mining and Geology

The Yuzhou main canal goes through 4 mined-out areas, namely, Xinfeng, Guocun, Gongmao and Fuli mined-out area, as shown in Figure 1 and Table 1. The mined-out areas are horizontally 3.11 km long. Most of the mined-out ar-

Table 1: Characteristics of mined-out areas along Yuzhou section of Middle Route Project.

Name	Area (m^2)	Occupation area of canal (m^2)	Length (m)	Thickness(m)	Depth (m)	Close-down date
Xinfeng	1387260	83314	724.98	0.9	107-266	1965
Guocun	525045	74772	703.46	0.75-1.13	126-290	1996
Gongmao	194086	71603	748.47	0.69-1.04	106-242	2005
Fuli	16389	16057	933.09	1-1.2	90-134	2003

Table 2: Ground fissures in the mined-out area.

Location	Number	Length (m)	Maximum width (m)	Visible depth (m)	Strike	Occurrence time
North Chenkou	3	≤ 30	0.3	≤ 1	WE	1960s
South Guocun	> 10	> 10	0.4	≤ 2	WE	1990s
Cichang	> 5	4.5-20	0.5-2.0	1.5-2.0	WE	1990s
Liudong-Dongcun	Unknown	≤ 80	0.3	≤ 1	Unknown	After rain in August, 2000

eas have one layer, a few areas have two layers, and each coal seam is about 1m thick. Most of mined-out areas were formed by small-scale coal mining after 1990s, and the mining has stopped since 2002. The mined-out areas are generally 100-269m deep, and a mobile basin occurs on the ground which is over 1700 m long in the WE direction and about 40m wide in the SN direction.

The study area is located in the southwest of North China Craton [14]. The terrain is generally flat, with above sea level of 123-145m in the transition zone between the alluvial apron and the plain. The coal measure strata are the Permian Shanxi formation and Shihezi formation with attitude of 195° < 14°.

The coal measure strata are monoclinic. The main faults in the area were formed before Quaternary, and Quaternary faults are not well developed. The largest fault is the Hutoushan Fault, which controls coalfield distribution. The fault is a normal fault with attitude of about 30° < 70°, but the fault plane is undulated. The faults are covered by loess, with fault throw of 117-427m.

The groundwater is 4-8m deep, and its flow direction is in compliance with slope of the terrain. Permian mudstone, shale, and Quaternary clay are good aquifuges, and there is no hydraulic connection between phreatic water and mines.

2.2 Characteristic and mechanism of Surface Deformation

After underground mining, the collapse, fracture and deformation of overlying rock mass happened due to the geological environment disruptions such as strata loss and stress field change, which then resulted in the subsidence, collapse fissures on the ground surface. There are both large and small coal mines in Yuzhou mining area. In the small mines, the fifth and sixth coal measures of upper Shihezi Formation formed in Permian were mined. The mining sequence and spaces did not match the specification requirements. Therefore, the movement and deformation on surface varied greatly, and there were many ground fissures in the mined-out area, as listed in Table 2. Most ground fissures are less than 5m deep, a few centimeters to more than ten centimeters wide, and less than 200m long, with strike of WE.

As we know, before mining, the rock mass was stable, and there were no any deformation or failure in the area. After mining, especially disordered mining or mining without support, initial in-situ stress field was destroyed, which caused some deformations and failures such as bending, breaking and caving. If the mining coal seam was shallow, or the deformation and failure of the wall rock was serious, they would influence ground surface, and caused subsidence, crack, tilt and horizontal displacement. With the enlargement of mined-out area, the defor-

mation and failure of ground surface would develop into a subsidence trough.

Occurrence, development and results of deformation and failure in mined-out area were controlled by mechanical properties and structure of upper strata. At the same time, position and occurrence of coal bed, depth, thickness and method of mining also influenced the deformation and failure.

Upper strata are soft rock with hard rock, and their strikes are generally along EW direction, with south dip and dip angle of 12-19°. The deformation of upper rock mass was a funnel-shaped subsidence from mining position to ground, and the deformed rock mass can be divided three zones: caving zone, fault zone, and bend zone, as shown in Figure 2.

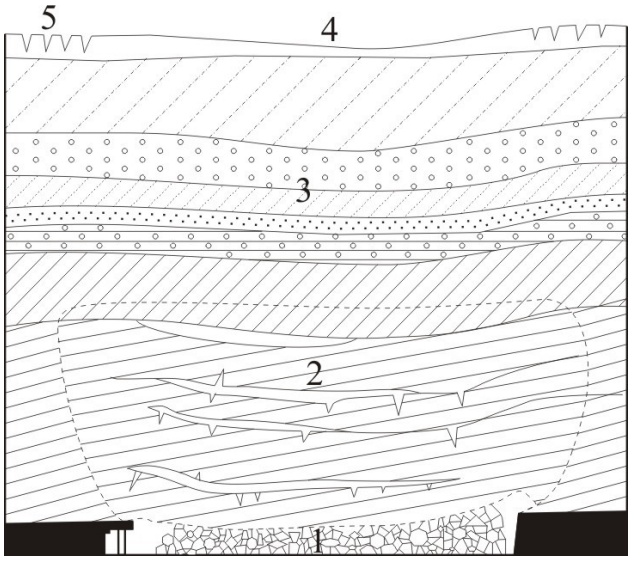

Figure 2: Model of deformation and failure in the mined-out area. 1-caving zone; 2-fault zone; 3-bend zone; 4- subsidence trough; 5-ground fissure.

Most ground fissures are found on the outer margin of the subsidence trough, and they were parallel to boundary of the mined-out area. The scale (including width, depth and length) of the ground fissures are closely related to the type, thickness, component, physical and mechanical properties of topsoil. Generally, when the surface tensile deformation value exceeds 6 to 10mm/m in large plastic clayey soil, the ground fissures would occur around the subsidence trough. In addition, the fractures will happen when the tension deformation on the ground surface is 2-3mm in sandy clay, clay sand or rock. The range of subsidence trough and ground fissures is larger than underground mined-out area.

The area of ground subsidence increases with depth of mining, and the depth of subsidence decreases with depth of mining.

3 Methodologies for subsidence prediction

3.1 Method of subsidence prediction

The probability integral method used to predict the subsidence is based on the random medium theory. The rock mass is considered to consist of a large number of loose granular media. During the movement of rock mass, its continuity was destroyed, and the original connection between the media units changes. The units separate and move relative to each other. The influence of the whole mining on rock strata and surface is equal to the sum of the influence of each unit mining on strata and surface. According to the random medium theory, the surface subsidence basin caused by unit mining is the normal distribution, and is consistent with the probability density distribution. The probability integration method considers the overburden subsidence due to the unit mining as a random event to describe the possibility of settlement and settlement of rock mass [15, 16]. The probability integral method has become one of the most mature and widely used methods in China, and it is used in this study [17–19].

Figure 3 shows the comparison between the ideal sinking curve and actual sinking curve. The $W'(x)$ represents the ideal limit settlement curve, and the $W(x)$ denotes the actual subsidence curve.

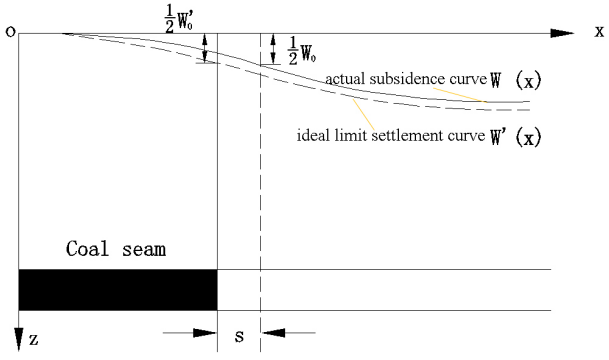

Figure 3: Comparison between ideal and actual subsidence curves.

The ideal limit subsidence curve is expressed as

$$W'(x) = \frac{q' m \cos\alpha}{2}\left[erf\left(\frac{\sqrt{\pi}}{r}x\right) + 1\right] \quad (1)$$

Table 3: Results of Surface subsidence distribution function.

x/r	0	±0.1	±0.2	±0.3	±0.4	±0.5	±0.6	±0.7
$W(x)/W_0$	0.500	0.599	0.692	0.744	0.842	0.895	0.934	0.961
	0.500	0.401	0.308	0.226	0.158	0.105	0.067	0.039
x/r	±0.8	±0.9	±1.0	±1.1	±1.2	±1.3	±1.4	±1.5
$W(x)/W_0$	0.978	0.988	0.994	0.997	0.998	0.999	0.999	0.999
	0.023	0.012	0.006	0.003	0.002	0.001	0.001	0.001

where $W'(x)$ is the ideal limit subsidence curve, q' is the limiting subsidence coefficient, obviously $q < q' \leq 1$, m is the goaf thickness, α is the dip angle of coal seam, $W'_0 = q'm\cos\alpha$ is the maximum settlement, r is the influence radius, $r=H/\tan\beta$, β is the influence angle of coal seam,x is the length of goaf, and *erf* is the probability integral function.

The actual surface subsidence curve is

$$W(x) = \frac{qm\cos\alpha}{2}\left[erf\left(\frac{\sqrt{\pi}}{r}(x-s)\right)+1\right] \tag{2}$$

where $W(x)$ is the actual subsidence curve, q is the current surface subsidence coefficient, and s is the offset of inflection point.

In the limit condition, the distribution curve of goaf surface subsidence is $W'(x)$, and q' in Formula (1) has the limit value of 1. The ultimate residual subsidence curve $W_0(x)$ is

$$We(x) = W'(x) - W(x). \tag{3}$$

The maximum residual settlement is the maximum of $W_e(x)$, which can be solved by Formula (3). Figure 2 shows that the most value point of $W(x)$ is at the right side of the S. Assuming that the maximum point of $W'(x)$ is at the point $x0$, and the point of the maximum value of $W(x)$ is x_0+S. According to Formula (3), the maximum value of $W(x)$ is between x_0 and x_0+S. The results of surface subsidence distribution function are listed in Table 3, which shows that, from the point $x0$ to the point x_0+S, the $W'(x)$ value decreases while the value of $W(x)$ increases. Therefore, $W_e(x)$ reaches the maximum value at the point x_0, which is shown by

$$We\max = W'0 - \eta W0 \tag{4}$$

where η is the reduction factor which can be determined in Table 3 by letting x/r=1-S/r.

The first order reciprocal and two reciprocal of the curve $W(x)$ are the tilt curve i_x and the curvature curve K_x, respectively. U_x is the horizontal displacement curve, and ϵ_x is the horizontal displacement curve. According to the literature [20], the maximum values are

$$i0 = \frac{W0}{r}, \tag{5}$$

$$K0 = 1.52\frac{W0}{r2}, \tag{6}$$

$$U0 = bW0, \tag{7}$$

where b is the horizontal movement coefficient,

$$\varepsilon 0 = 1.52\frac{bW0}{r}, \tag{8}$$

where W_0 is the maximum residual settlement of actual settlement curve.

The substitute of maximum residual settlement value into equations (5) - (8) will result in the corresponding residual deformation.

3.2 Deformation monitoring

In order to correctly evaluate the stability of the mined-out areas and their influence on the section of the Diversion Project and other buildings, a high precision deformation observation network (including surface leveling and horizontal deformation observation) was installed along the channel (Figure 1).

The observation network covers 4 mined-out areas, namely, Xinfeng, Guocun, Gongmao and Fuli mined-out areas.

Deformation observation sections are set up every 100 to 200m along the center line of the channel. Each observation section has three deformation monitoring points, one in the center of the canal and two at two sides 50-150m from the canal center. Therefore, there are 33 deformation monitoring points in total. In addition, there are 3 vertical working bench marks and 3 horizontal working bench marks (Figure 1).

The datum network should be rechecked every six months, and the points should be observed every a month. If there were special factors, time interval could vary.

Table 4: Parameters for mined-out area subsidence prediction by probability integral method.

Names	Definition	Values
Subsidence coefficient	When fully mining, the ratio of the maximum subsidence value of the ground surface to the projection length of the normal thickness of the coal seam in the vertical direction.	0.03
Horizontal movement coefficient	When fully mining, the ratio of the maximum horizontal movement of the surface to the maximum subsidence value on the main section	0.35
Tangent of major influence angle	The ratio of mining depth to the main influence radius	1.8
Displacement distance of inflection point	the distance between the inflection point of the sinking curve and the coal wall	0(m)
Coal seam thickness	-	2(m)

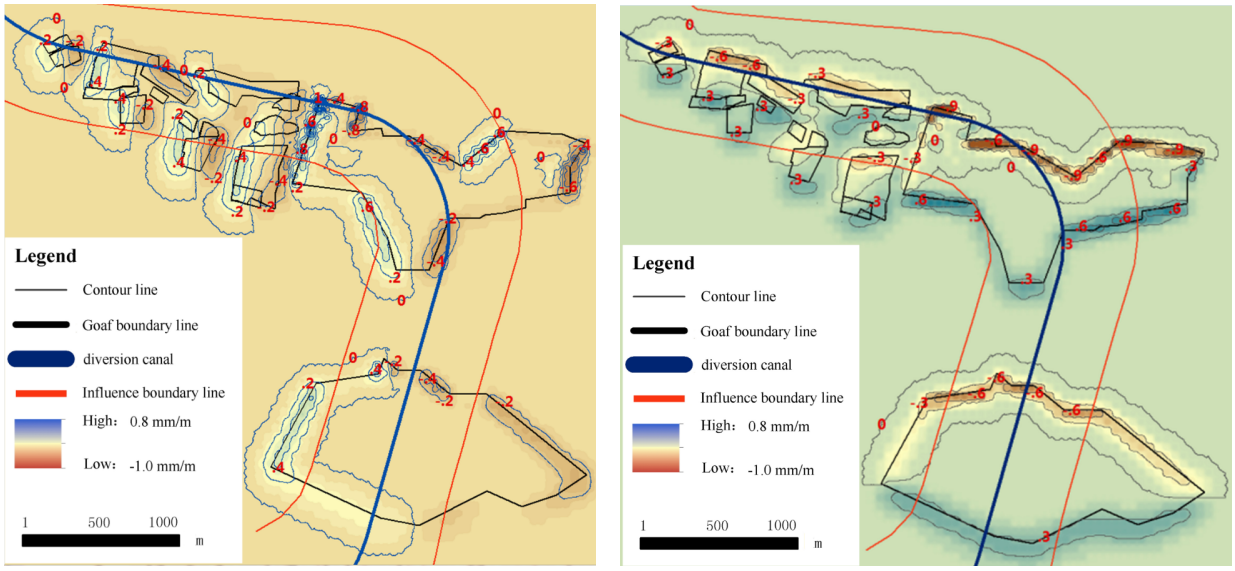

(a) Prediction results along strike direction

(b) Prediction results along dip direction

Figure 4: Tilt distribution.

Table 5: Prediction results of maximum subsidence in different horizontal plane (mm).

horizontal plane	Guocun	Xinfeng	Gongmao	Fuli
Ground surface	60	60	54	42
Underground 50m	110	110	100	80
Underground 100m	200	225	175	150
Underground 150m	320	320	280	200

3.3 Prediction parameters

The prediction parameters generally include the coal seam thickness, subsidence coefficient, horizontal movement coefficient, tangent of major influence angle, uphill inflection point offset, downhill inflection point offset and influence propagation angle coefficient. According to the *code for building, water body, railway and main well roadway pillar retention and pressure coal mining* [19] and measured data, the parameters are listed in Table 4.

The subsidence coefficient is calculated with the following formula (9). Because the prediction is the residual displacement deformation of the mined-out areas, and the mined-out areas were grouted to reduce subsidence, the

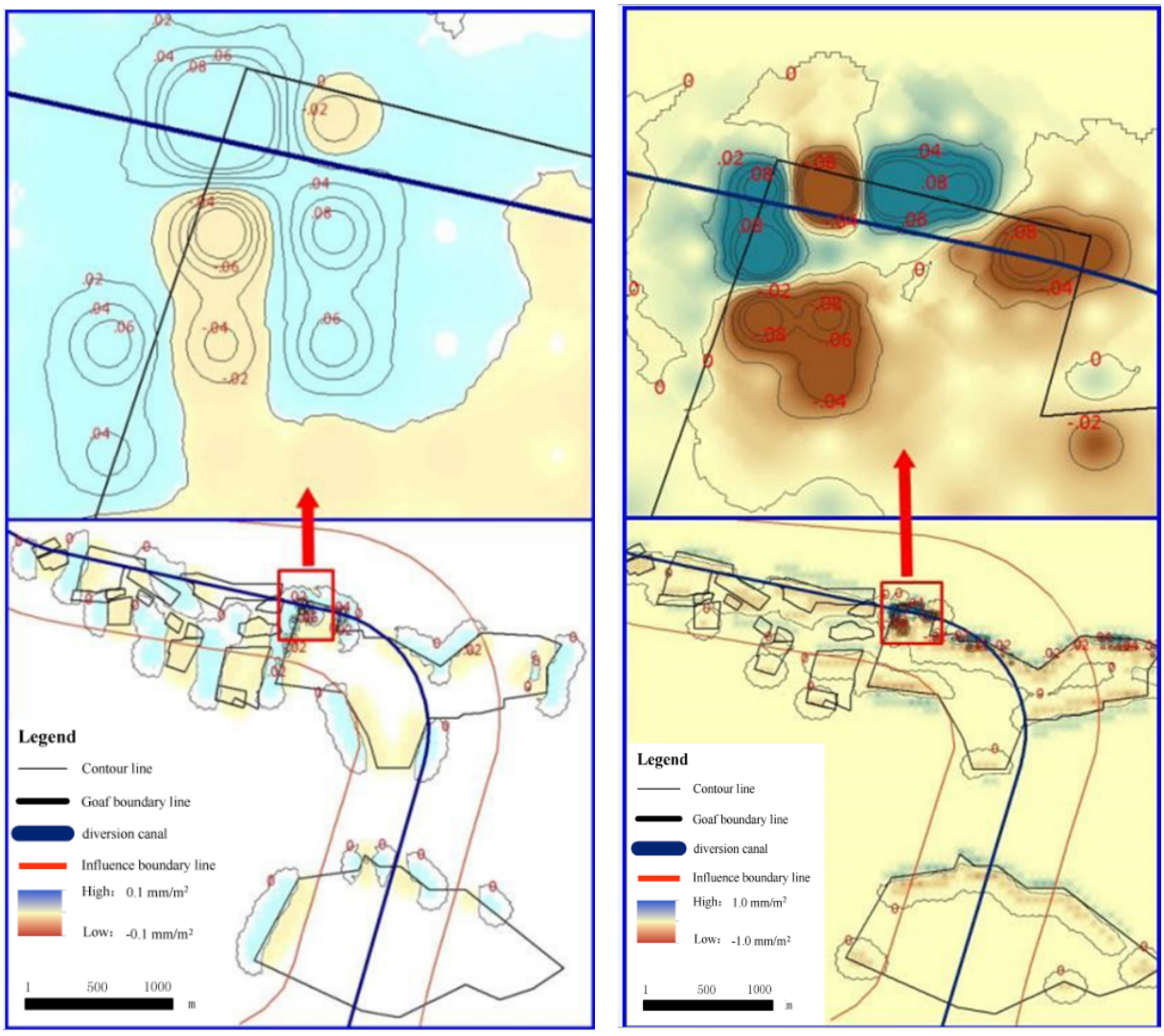

(a) Prediction results along strike direction

(b) Prediction results along dip

Figure 5: Surface curvature distribution.

subsidence coefficient is relatively small.

$$q_1 = (1 - q) \times (1 - q_2), \tag{9}$$

where, q_1 is the surface residual subsidence coefficient after grouting, q is the surface subsidence coefficient (q = 0.88 here according to *Code for coal mining under buildings, water-bodies and railways* [19]), and q_2 is the effect of grouting.

3.4 Prediction results

The ground tilt prediction results along strike are shown in Figure 4(a), with maximum negative tilt of -0.8 mm/m at the northwest corner of Guocun mined-out area and maximum positive tilt of 0.6 mm/m at the southwest and north of Guocun mined-out area and the North and southwest of the Xinfeng mined-out area, which is under the channel.

The ground tilt prediction results along dip direction are shown in Figure 4(b), with maximum negative tilt of −0.9 mm/m at the northwest corner of Guocun mined-out area and maximum positive tilt of 0.6 mm/m at southwest and north of Guocun mined-out area, which is just under the channel.

The predicted results of surface curvature are shown in Figure 5, with maximum negative curvature of −0.08 mm/m^2 and maximum positive curvature of +0.08 mm/m^2 at the northwest corner of Guocun mined-out area, which is just under the channel.

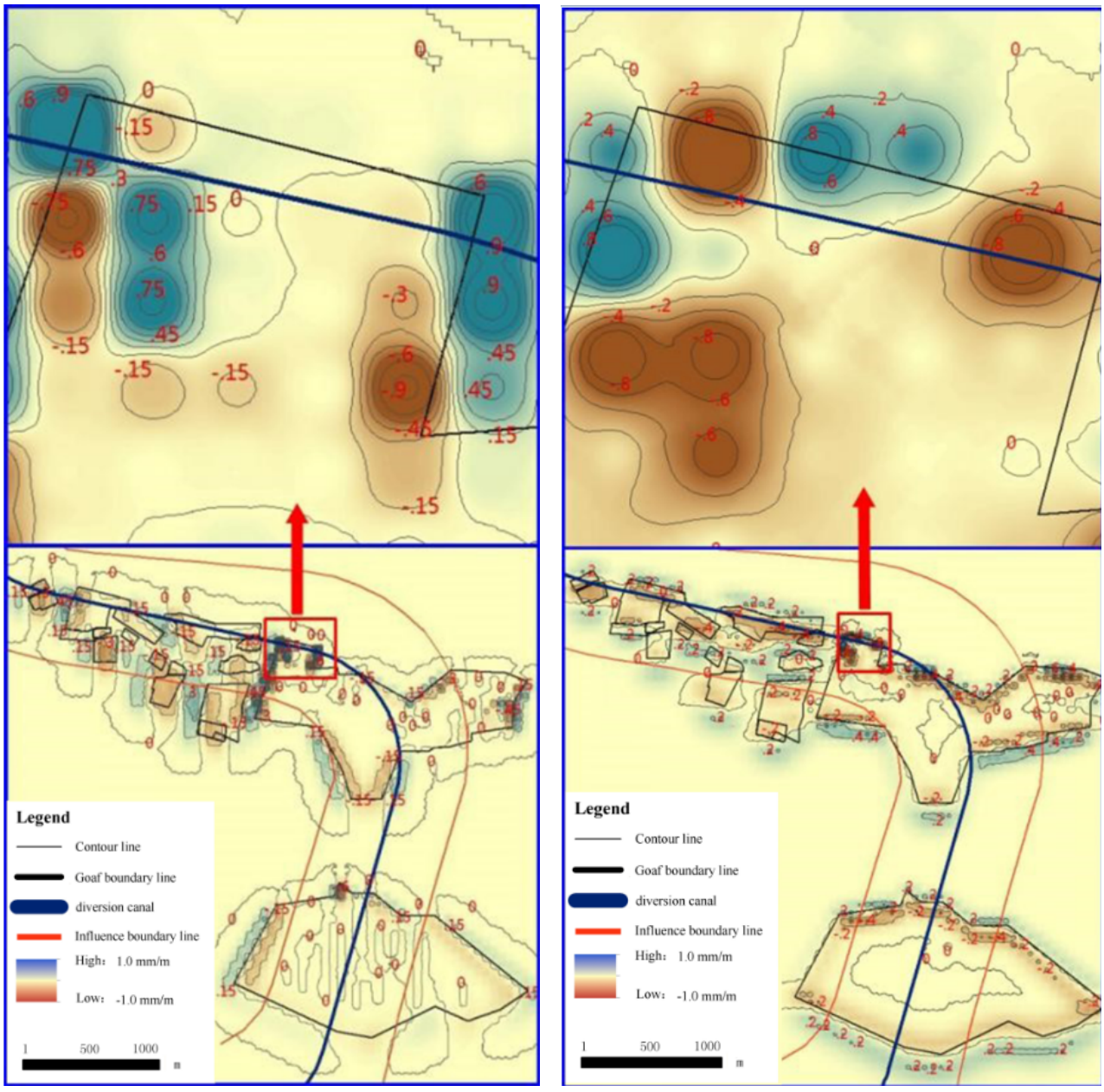

(a) Prediction results along strike direction

(b) Prediction results along dip direction

Figure 6: Distribution of horizontal deformation.

The predicted results of horizontal surface deformation are shown in Figure 6, with maximum negative horizontal deformation of −0.9 mm/m and maximum positive horizontal deformation of 0.9 mm/m at the northwest corner of Guocun mined-out area, which is just under the channel.

According to the *code for building, water body, railway and main well roadway pillar retention and pressure coal mining* [19], the allowable deformation of ground surface is: tilt $i = \pm 3$mm/m, curvature $K = +0.2\times10^{-3}$/m, horizontal deformation $\epsilon = +2$mm/m. Therefore, the channel will not be destroyed in terms of the ground deformation.

The prediction results of subsidence for the surface, −50m, −100m and −150m are shown in Figure 7. It can be found from Table 4 that the subsidence increases with depth. The position with maximum subsidence of Guocun and Xinfeng mined-out areas are under the channel. However, the distance from the position with maximum subsidence of Fuli mined-out area to the channel is far.

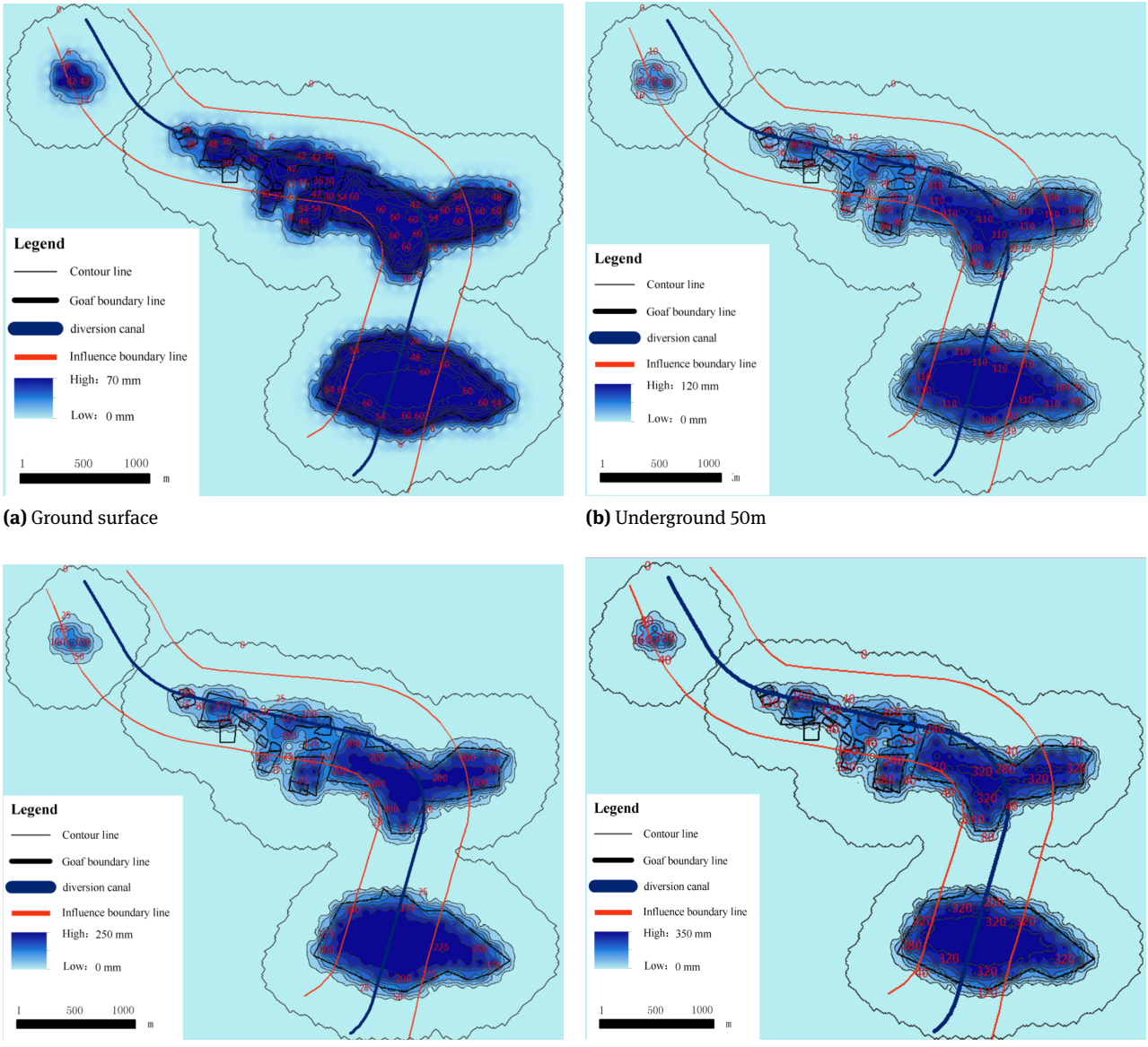

(a) Ground surface

(b) Underground 50m

(c) Underground 100m

(d) Underground 150m

Figure 7: Contour of subsidence.

4 Conclusion and discussions

There were four mined-out areas along Yuzhou section of Middle Route Project of South-to-North water diversion. The collapse, fracture and deformation of overlying rock mass occurred due to strata loss and stress field change, which then resulted in the subsidence, collapse fissures on the ground.

The geological structure follows the typical "three-zone" overlying rock failure, and then the surface deformation and the underground failure are also the same as that of the "three-zone" overlying rock failure. Therefore, the deformation of the upper rock mass was a funnel-shaped subsidence from mining position to ground can be divided three zones: caving zone, fault zone, and bend zone.

According to the monitoring data, the surface tilt, curvature and horizontal deformation of the mined-out areas were less than critical values specified by the *Code for coal mining under buildings water-bodies and railways*. Therefore, the channel will not be destroyed in terms of the ground deformation.

The prediction of the internal subsidence of overlying rock shows that the subsidence increases with depth. The

forecast and monitoring values are relatively larger in Guocun and Xinfeng mined-out areas, because the two mined-out areas are large and sufficient mining degree is high. Furthermore, their continuous deformation will affect the safety of the channel. Therefore, the two mined-out areas should be the focus of monitoring. Based on the prediction results, the classification pre-warning system model can be built for the channel.

Acknowledgement: This study was supported by the PhD student innovation fund of North China University of Water Resources and Electric Power and the National Natural Science Foundation of China (U1704243 & 41741019).

References

[1] Dron R. W., Effect of Coal Workings on the Surface. Jour. Brit. Soc. Min. Stud., 1889, 11, 122

[2] Can E., Kuşcu Ş., Kartal M. E., Effects of mining subsidence on masonry buildings in Zonguldak hard coal region in Turkey. Environmental Earth Sciences, 2012, 66(8), 2503-2518

[3] Can E, Kuşcu Ş., Mekik C. Determination of underground mining induced displacements using GPS observations in Zonguldak-Kozlu Hard Coal Basin. International Journal of Coal Geology, 2012, 89(1), 62-69.

[4] Donnelly L. J., Cruz H. D. L., Asmar I., Zapata O., Perez J.D., The monitoring and prediction of mining subsidence in the Amaga, Angelopolis, Venecia and Bolombolo Regions, Antioquia, Colombia. Engineering Geology, 2001, 59(1–2), 103-114

[5] Gayarre F. L., Álvarez-Fernández M. I., González-Nicieza C., Álvarez-Vigil A.E., García G.H., Forensic analysis of buildings affected by mining subsidence. Engineering Failure Analysis, 2010, 17(1), 270-285

[6] Nádudvari Á., Using radar interferometry and SBAS technique to detect surface subsidence relating to coal mining in Upper Silesia from 1993-2000 and 2003-2010. Environmental & Socio-economic Studies, 2016, 4(1), 24-34

[7] Howladar M. F., Hasan K., A study on the development of subsidence due to the extraction of 1203 slice with its associated factors around Barapukuria underground coal mining industrial area, Dinajpur, Bangladesh. Environmental Earth Sciences, 2014, 72(9), 3699-3713

[8] Jung Y. B., Song W. K., Cheon D. S., Lee D. K., Park J. Y., Simple method for the identification of subsidence susceptibility above underground coal mines in Korea. Engineering Geology, 2014. 178, 121–131

[9] Hu Z., Chen C., Xiao W., Wang X., Gao M., Surface movement and deformation characteristics due to high-intensive coal mining in the windy and sandy region. Int. J. Coal Sci. Technol, 2016, 3(3), 339-348

[10] Sun Y., Zhang X., Mao W., Xu L., Mechanism and stability evaluation of goaf ground subsidence in the third mining area in Gong Changling District, China. Arabian Journal of Geosciences, 2015, 8(2), 639-646

[11] Li H., Zhao B., Guo G., Zha J., Bi J., The influence of an abandoned goaf on surface subsidence in an adjacent working coal face: a prediction method. Bulletin of Engineering Geology & the Environment, 2016, 1-11

[12] Liu H., Zhu H., Huang Y., Stability research Guocungoaf at Middle Route Project on area of South-to-North water diversion. Rock and Soil Mechanics, 2015, 36(S2), 519-524 (in Chinese with English summary)

[13] Wu D., Ni H., Overview on design and key technological problems of Middle Route Project of South - to - North Water Diversion. Yangtze River, 2014, 6, 1-3 (in Chinese with English summary)

[14] Lin D., Pei F., Li X., Zuo A., Regional Geological Survey of Henan Province. Regional Geology of China, 1998, 17(4), 337-346 (in Chinese with English summary)

[15] He G., Yang L., Ling G., Mining subsidence. China University of Mining and Technology Press, Xuzhou, 1991 (in Chinese)

[16] Han X., Meng X., Zhang X., Zhang Y., The Deformation Stability Analysis of the Tunnels in Mined-out Areas Based on Creator and FLAC^{3D}. Journal of Water Resources and Architectural Engineering, 2014, 12(5), 93-97 (in Chinese with English summary)

[17] Liu B., Dai H., Research Development and Origin of Probability Integral Method. Coal Mining Technology, 2016, 21(2), 1-3 (in Chinese with English summary)

[18] Wang S., Prediction method of rock layer and surface movement. China Coal Industry Publishing House, Beijing, 1989 (in Chinese)

[19] China State Coal Industry Administration, code for building, water body, railway and main well roadway pillar retention and pressure coal mining. Coal Industry Press, Beijing, 2017 (in Chinese)

[20] Xie H., Zhou H., Wang J., Li L., Kwasniewski M.A., Application of flac to predict ground surface displacements due to coal extraction and its comparative analysis. Chinese Journal of Rock Mechanics and Engineering, 1999, 18(4), 397-401 (in Chinese with English summary)